

# A Structural Reconsideration: Linear Aliphatic or Alicyclic Hard Segments for Biodegradable Thermoplastic Polyurethanes?

Konstanze Seidler,<sup>1,2</sup> Katharina Ehrmann,<sup>1,2</sup> Patrick Steinbauer,<sup>1,2</sup> Andreas Rohatschek,<sup>3,2</sup> Orestis G. Andriotis,<sup>3,2</sup> Claudia Dworak,<sup>1,2</sup> Thomas Koch,<sup>4</sup> Helga Bergmeister,<sup>5,6,2</sup> Christian Grasl,<sup>5,7</sup> Heinrich Schima,<sup>5,7</sup> Philipp J. Thurner,<sup>3,2</sup> Robert Liska,<sup>1,2</sup> Stefan Baudis <sup>1,2</sup>

<sup>1</sup>Institute of Applied Synthetic Chemistry, Division of Macromolecular Chemistry, TU Wien, Getreidemarkt 9/163 MC, 1060, Vienna, Austria

<sup>2</sup>Austrian Cluster for Tissue Regeneration, 1200, Vienna, Austria

<sup>3</sup>Institute of Lightweight Design and Structural Biomechanics, TU Wien, Getreidemarkt 9/317, 1060, Vienna, Austria

<sup>4</sup>Institute of Materials Science and Technology, TU Wien, Getreidemarkt 9/308, 1060, Vienna, Austria

<sup>5</sup>Ludwig Boltzmann Cluster for Cardiovascular Research, Währinger Gürtel 18-20, 1090, Vienna, Austria

<sup>6</sup>Center for Biomedical Research, Medical University of Vienna, Währinger Gürtel 18-20, 1090, Vienna, Austria

<sup>7</sup>Center for Medical Physics and Biomedical Engineering, Medical University of Vienna, Währinger Gürtel 18-20, 1090, Vienna, Austria

Correspondence to: S. Baudis (E-mail: stefan.baudis@tuwien.ac.at)

Received 30 April 2018; Accepted 9 July 2018; published online 9 September 2018

DOI: 10.1002/pola.29190

**ABSTRACT:** Thermoplastic polyurethane elastomers (TPUs) with a biodegradable chain extender and different nonaromatic diisocyanate hard segments were synthesized and tested concerning their thermal, mechanical, and degradation properties and for their processability regarding electrospinning. The design of the TPUs was based on the structural modification of the hard segment using linear aliphatic hexamethylene diisocyanate (HMDI), more rigid alicyclic 4,4'-methylene bis(cyclohexylisocyanate) (H12MDI), 1,3-bis(isocyanatomethyl)cyclohexane (BIMC), or isophorone diisocyanate (IPDI). The soft segment consisted of poly(tetrahydrofuran). Bis(2-hydroxyethyl) terephthalate (BET) was used as chain extender with cleavable ester bonds. Some of the polyurethanes

based on alicyclic diisocyanate showed better mechanical performance than the less rigid HMDI-based TPU. The TPU *in vitro* degradability was tested for 25 days at elevated temperatures in PBS buffer and indicated a bulk erosion process. Electrospinning experiments were conducted and promising results with respect to further applicability of these materials in vascular tissue engineering were obtained. © 2018 The Authors Journal of Polymer Science Part A: Polymer Chemistry Published by Wiley Periodicals, Inc. *J. Polym. Sci., Part A: Polym. Chem.* **2018**, *56*, 2214–2224

**KEYWORDS:** biodegradable; electrospinning; nontoxic; thermoplastic polyurethane; vascular grafts

**INTRODUCTION** Tissue engineering (TE) is an interdisciplinary research field, consisting mainly of medicine, biology, chemistry, and mechanical engineering. The primary aim of TE is to repair damaged tissue and organs by using artificial tissues or tissue replacements, produced either *in vitro* or *in vivo*.<sup>1–5</sup> Herein, the scaffold plays a key role for the regeneration of tissue. It is usually a biodegradable, porous construct, which acts as a temporary support for the new formed tissue. The scaffold can be made of either an inorganic or organic biomaterial or a combination of both in form of composites. Scaffolds may consist of gels, sponge-like sheets, or highly complex structures with intricate pores or channels, maintaining two primary functions by mimicking the extracellular matrix (ECM): providing the necessary mechanical support and form a protective barrier to the wounded area. In

our research, we are engaged in the synthesis and characterization of polymers that can be used to manufacture scaffolds for vascular tissue engineering (VTE) using electrospinning processes.<sup>6–9</sup> Numerous studies focus on the development of substitutes for small-diameter vessels, which mimic the microstructure of native tissue and its physical characteristics. Through electrospinning (ES), it is possible to produce seamless, nonwoven fibrous structures with graft walls consisting of a web of randomly oriented micro- to nanofibers with an architecture mimicking the ECM by having a large surface-to-volume ratio and high porosities with interconnected pores.<sup>10–13</sup>

Biodegradability plays a central role for VTE and is usually based on the hydrolytic cleavage of polymer moieties.

© 2018 The Authors Journal of Polymer Science Part A: Polymer Chemistry Published by Wiley Periodicals, Inc.

This is an open access article under the terms of the Creative Commons Attribution NonCommercial License, which permits use, distribution and reproduction in any medium, provided the original work is properly cited and is not used for commercial purposes.

[Corrections added on 15 March 2019 after first online publication: Copyright line has been corrected]

Therefore, polyester-based scaffolds like poly(glycolic acid), poly(lactic acid), or poly( $\epsilon$ -caprolactone), copolymers, or blends thereof were often used for biodegradable electrospun grafts in the past.<sup>14</sup> However, their biomechanical properties were mostly poor and relatively thick graft walls or multilayered scaffolds have to be applied with these materials to ensure sufficient stability.<sup>15</sup> Also scaffolds derived from natural materials, like allografts or xenografts, have been investigated for VTE, but they often provoke immune response in spite of being decellularized.<sup>16,17</sup> Additionally, protein<sup>18–20</sup> or polysaccharide based<sup>21–23</sup> biomaterials have been used in different studies for VTE, but poor mechanical properties of these materials are often the cause for failure.

Among the synthetic biomaterials used for VTE, thermoplastic urethane elastomers (TPUs) have proven to be the most promising biomaterials owing to their excellent elasticity and biocompatibility. In contrast to aforementioned polyesters, they consist of a block copolymer structure resulting from the polyaddition reaction of macrodiols with diisocyanates (Fig. 1). Several factors are known to influence the final properties of thermoplastic polyurethanes, mainly by affecting the microphase separation: These include polymerization method, hard segment composition with special respect to concentration, and diisocyanate type and symmetry. The nature and flexibility of the chain extender affects hydrogen bonding.<sup>24</sup>

Segmented TPUs are composed of consecutive hard segments and soft segments, causing the above-mentioned microphase separation, which leads to the formation of immiscible ordered (up to crystalline) and rather amorphous domains. Interchain hydrogen bonding between urethane groups helps to stabilize the ordered domains. In contrast to that, the predominantly amorphous soft segments consist of flexible polyester, polyether, or polysiloxane chains.<sup>26</sup> This specific polymer architecture of TPUs with hard and soft segments results in nonlinear mechanical properties with superior elasticity in contrast to the aforementioned polyester-based materials.

The desired mechanical properties for artificial grafts are low elastic moduli comparable to the natural blood vessel (in the

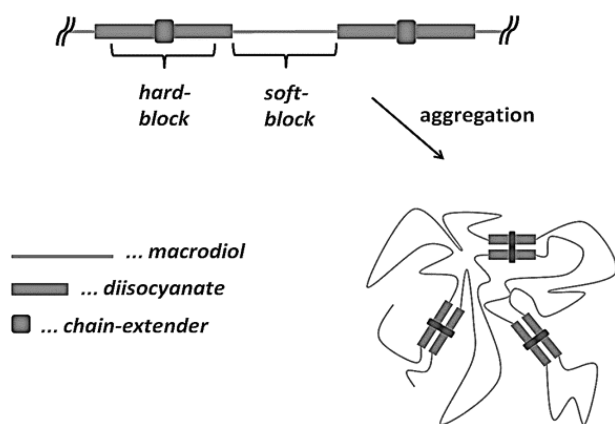


**FIGURE 1** Polymer architecture of TPUs, single polymer chain (top) and aggregation (bottom).<sup>25</sup>

range of 500 kPa), combined with a high strength (above 1000 kPa). Recently, we developed a thermoplastic polyurethane polymer containing a cleavable chain extender (CE). Grafts out of this TPU can be fabricated by ES and display biomechanical properties similar to the FDA approved, nondegradable TPU Pellethane<sup>®</sup> (Lubrizol Trademark).<sup>25</sup> Biomechanical characterization consisting of tensile testing (compliance, tensile strength), suture retention strength, and *in vitro* cell studies of the electrospun grafts revealed suitable mechanical properties and nontoxic degradation products. A follow-up *in vivo* study with a small rodent model<sup>27</sup> on the applicability of this TPU for small-diameter vessel substitutes showed its suitability for thin-walled prostheses, very good long-term performance, and resistance to biomechanical failures. Nevertheless, a higher strength would be desirable, as the load with respect to blood pressure increases with larger vessel diameters in large animal models. Besides, higher strength is also expected to influence the suture tear resistance of the material in a positive way.

The polymer structure, morphology, and crystallinity of the hard segment in TPUs depend on the structure of the used diisocyanate (DI) and hence have an impact on the mechanical properties of the polymer.<sup>24,28</sup> In this study, we considered the modification of hard segment structure by variation of the used DI, leaving the type of soft segment and chain extender constant. However, aromatic isocyanates, which are mainly the basis for commercial high-performance TPUs, are problematic as their corresponding amines are known to be toxic<sup>29,30</sup> and should therefore not be considered as precursor for biodegradable polymers for TE applications. For this reason, methane-4,4-diphenyl diisocyanate (MDI) was substituted by linear aliphatic hexamethylene diisocyanate (HMDI, Fig. 2) in a previous study.<sup>25</sup> The introduction of alternative aromatic moieties into the hard segments using the terephthalate-based chain extender bis(2-hydroxyethyl) terephthalate (BET, Fig. 2), which exhibits no toxic metabolites, partially compensated the loss of mechanical stability caused by the exclusion of MDI. However, the tensile strength of electrospun grafts was only about 50% of the commercial benchmark Pellethane<sup>®</sup>.<sup>25</sup>

Herein, we extended the material portfolio by including TPUs synthesized from commercial alicyclic diisocyanates. That is, apart from the flexible linear aliphatic hexamethylene diisocyanate (HMDI) hard segment, more rigid alicyclic diisocyanates were investigated (Fig. 2): 4,4'-methylene bis(cyclohexyl isocyanate) (H12MDI) was chosen due to its structural similarity to methane 4,4'-diphenyl diisocyanate (MDI), which is used as hard segment in the nondegradable benchmark material Pellethane<sup>®</sup>. In addition to H12MDI, also 1,3-bis(isocyanatomethyl)cyclohexane (BIMC) and isophorone diisocyanate (IPDI) offer easy availability and new structural aspects. IPDI shows a more sterically hindered structure and less symmetry if compared to H12MDI and BIMC due to the methyl groups and provides one primary and one secondary isocyanate group.

The decreased chain flexibility of alicyclic DIs compared to linear aliphatic ones was proposed to increase modulus and tensile strength. In general, diisocyanate chain symmetry is an important factor for the hard segment structure of TPUs.<sup>24</sup> Polymers with two symmetrical diisocyanate moieties in the

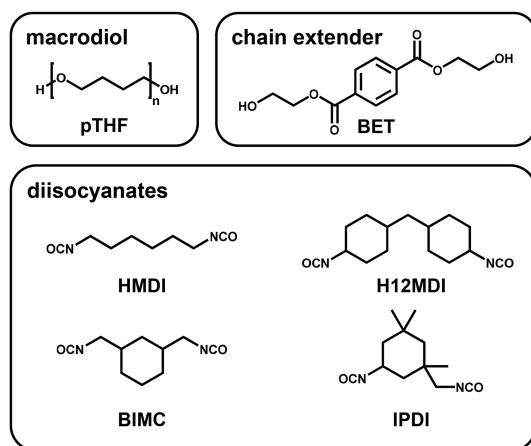


**FIGURE 2** Structures of the thermoplastic polyurethane segments used in this study: poly(tetrahydrofuran) (pTHF), bis(2-hydroxyethyl) terephthalate (BET), hexamethylene diisocyanate (HMDI), 4,4'-methylene bis(cyclohexyl isocyanate) (H12MDI), 1,3-bis(isocyanatemethyl)cyclohexane (BIMC), and isophorone diisocyanate (IPDI).

hard segment, regardless of aromatic or aliphatic origin, display higher crystallinity and hence higher strength. The conformational isomers of cyclohexyl ring moieties decrease hard segment crystallinity,<sup>31</sup> still in literature it is reported that TPUs synthesized from H12MDI have higher tensile strengths compared to polymers derived from HMDI or IPDI with the same hard segment content.<sup>28</sup> We were interested in how these effects affect the properties of biodegradable TPUs and therefore we investigated the properties of the polymers synthesized with different diisocyanates with a steadily decreasing symmetry: HMDI > H12MDI > BIMC > IPDI.

All aforementioned TPUs were synthesized and characterized by their molecular weight (gel permeation chromatography, GPC), thermomechanical properties (tensile test; differential scanning calorimetry, DSC; dynamic mechanical thermal analysis, DMTA), hydrolytic degradation, and water uptake, respectively. Additionally, tubular grafts were prepared from selected TPUs by electrospinning and tested for their tensile properties compared to the nondegradable benchmark material Pellethane<sup>®</sup>.

## EXPERIMENTAL

### Materials

All chemicals and solvents were purified by means of standard laboratory methods<sup>32</sup> unless noted otherwise. Extra dry dimethylformamide (DMF, water content <50 ppm) for the polymer synthesis was purchased from Acros (Fisher Scientific Austria GmbH, Vienna, Austria). Poly(tetrahydrofuran) (pTHF) ( $\overline{M}_n = 1000 \text{ g mol}^{-1}$  confirmed by OH group titration according to DIN 53240), bis(2-hydroxyethyl) terephthalate (BET), tin (II) 2-ethylhexanoate ( $\text{SnOct}_2$ ), and all diisocyanates were purchased from Sigma Aldrich (Vienna, Austria).

The water content of the reactants was quantified by Karl-Fischer titration. All chemicals used for TPU syntheses (esp. the macrodiols) had a maximum water content of 50 ppm.

Pellethane<sup>®</sup> 2363-80A (Pell) was obtained from Lubrizol (Cleveland, OH) and used as a benchmark material for electrospun grafts for VTE.<sup>11,33</sup> Surgical PLA (poly(L-lactide-co-D,L-lactide)-copolymer with a molar L-lactide: D,L-lactide ratio of 85:15 (Resomer<sup>®</sup> RG, Sigma Aldrich, Vienna, Austria) was used as an additional reference for degradation experiments. PLA reference had a  $T_g$  of 57 °C (DSC). The molecular weight ( $\overline{M}_n$ ) according to GPC measurements (see below) was 152 kDa with a polydispersity of 1.53.

### Polymer Synthesis

The synthesis of the TPUs with degradable hard segment was performed as described in a previous study.<sup>25</sup> Briefly, the macrodiol pTHF was dried by stirring it at 90 °C under vacuum (4 mbar) for 48 h. Subsequently, for TPUs with a ratio diisocyanate (DI):macrodiol (MD):chain extender (CE) 2:1:1 or 3:1:2, dry pTHF (5 mmol) was weighed into a predried flask with mg accuracy. Drying was continued for another period of 48 h under the same conditions as above. DI (HMDI, H12MDI, BIMC or IPDI) (10 mmol or 15 mmol) was added in 3 mL dry DMF under a gentle nitrogen counter flow. The transfer needle and weighing vessel were rinsed with additional dry DMF. Finally, about 150  $\mu\text{L}$  of  $\text{SnOct}_2$  catalyst were added to the reaction mixture and the mixture was stirred at 50 °C for 3 h.<sup>34,35</sup> After cooling, the CE (5 mmol or 10 mmol) was added in 5 mL of dry DMF with subsequent rinsing of transfer needle and weighing flask. Finally, the reaction mixture was stirred overnight at 100 °C. The viscous mixture was diluted with 25 mL of DMF and the polymer was precipitated into 800 mL of methanol. The raw product was reprecipitated twice from tetrahydrofuran (THF) in methanol and dried at 50 °C *in vacuo*. The TPUs were obtained in yields above 80% (th.). The polymer names used throughout the whole manuscript follow the following systematic: DI\_[ratio DI:MD:CE], for example, HMDI\_211 refers to a polyurethane synthesized with HMDI with a ratio of DI:MD:CE of 2:1:1.

### Polymer Characterization

Molecular weight of the polymers was determined by gel permeation chromatography (GPC) measurements using a Viscotek<sup>®</sup> GPCmax VE2001 system with a refractive index (RI) detector (VE3850) and three columns (Waters Styragel<sup>®</sup> HR 0.5 THF, Waters Styragel<sup>®</sup> HR 3 THF and Waters Styragel<sup>®</sup> HR 4 THF) (Waters GmbH, Eschborn, Germany) with dry THF as mobile phase (1.0 mL  $\text{min}^{-1}$  flow rate) at 40 °C. The TPUs were dissolved in dry THF, filtered through a 0.2  $\mu\text{m}$  poly(tetrafluoroethylene) (PTFE) disposable Chromafil<sup>®</sup> 0-20/15MS syringe filter. The injection volume was 100  $\mu\text{L}$ . Calibration was performed with polystyrene standards ( $\overline{M}_n$  range between 0.370 and 177 kDa). Empower<sup>™</sup> Pro Software was used for the determination of the number average and weight average molecular weight ( $\overline{M}_n$  and  $\overline{M}_w$ ) to calculate the polydispersity  $D$  ( $\overline{M}_w/\overline{M}_n$ ).

For thermal and mechanical testing, polymer films were prepared as follows: the films were produced by solution casting from 10 wt % solutions of the TPUs in DMF in PTFE molds (60 × 40 × 0.2 mm<sup>3</sup>). The molds were then placed in an oven

for 48 h at 37 °C and the films were finally dried *in vacuo* at room temperature for 48 h.

Differential scanning calorimetry (DSC) experiments were performed on a TA instruments Q2000™ apparatus (TA instruments, Eschborn, Germany). Small pieces of the solution cast films were cut and weighed into aluminum pans. The experimental temperature ranged from 0 °C to 100 °C with a heating rate of 10 K min<sup>-1</sup> under nitrogen atmosphere.

Atomic force microscopy (AFM) experiments were performed on a NanoWizard® ULTRA SpeedA AFM system (JPK Instruments AG, Berlin) equipped with an inverted optical microscope (Axio Observer.D1, ZEISS). Nanomechanical assessment was performed via AFM cantilever-based nanoindentation experiments using a 4XC-NN rectangular cantilever (6.6 N m<sup>-1</sup> measured spring constant; μMasch, OPUS™) equipped with a sharp tip (nominal tip radius ~10 nm). The cantilever spring constant was calibrated with the thermal noise method<sup>36</sup> and the deflection sensitivity was obtained by performing 16 force measurements on the glass surface next to the sample, as previously described.<sup>37</sup> A 3 μm × 3 μm region of interest was scanned in Quantitative Imaging mode (QI™, JPK) with a maximum applied force of 20 nN and spatial resolution of 128 × 128 pixels to spatially resolve the indentation modulus. This results in 16,384 force indentation curves, mapped over the region of interest, which were analyzed to obtain the indentation modulus. The indentation modulus was calculated by employing the Hertz analysis method<sup>38</sup> and assuming the tip shape to be a paraboloid with a tip radius of 10 nm.

Tensile testing was performed on a Zwick Z050™ machine (Zwick GmbH & Co. KG, Ulm, Germany) with a 100 N load cell and a crosshead speed of 50 mm min<sup>-1</sup>. Each experiment was carried out in quintuplicate. The tensile tests were performed according to ISO 527-1 type 5B and the specimens were punched out of polymer films made by solution casting.

Dynamic mechanical thermal analysis (DMTA) measurements were carried out on a TA Instruments 2980 DMA™ apparatus (TA instruments, Eschborn, Germany). Rectangular specimens (20 × 2 mm<sup>2</sup>) with a thickness of about 200 μm were cut from the solution cast films as described above. The temperature range was set from -100 °C to 40 °C with a dwell period of 15 min, a heating rate of 3 K min<sup>-1</sup>, a frequency of 1 Hz, an amplitude of about 1.5 μm (0.1% of clamping distance), and a static force of 0.020 N. All experiments were performed in triplicate.

Hydrolytic degradation behavior and water uptake was investigated using thin films of each TPU, which were prepared by solution casting. Polymer films were punched into circular discs and weighed individually into vials (initial weight,  $m_0 = 11.5 \pm 4.5$  mg). Weight consistency was checked by another drying period of 48 h (as described above). Subsequently, the vials were filled with 10 mL of phosphate buffered saline solution (PBS, pH 7.4) and stored in an oven at 90 °C (± 3 °C) over a 25-day period. Samples were extracted at different time points ( $t$ ). The extracted samples were

washed twice with deionized water to remove PBS salts, dried with a paper towel, weighed (wet/swollen weight at  $t$ ,  $m_{w,t}$ ), vacuum dried at 45 °C for at least 48 h (until weight consistency), and weighed again (dry weight at  $t$ ,  $m_{d,t}$ ). GPC measurements were conducted to determine the molecular weight ( $M_t$ ) of selected samples. The remaining mass ratio at  $t$  ( $m_{r,t}$ ) and the remaining molecular weight ratio ( $M_{r,t}$ ) were calculated according to eqs 1 and 2 using the initial weight  $m_0$  and the initial molecular weight  $M_0$ , respectively. The water uptake ( $W$ ) was calculated by eq. 3.

$$m_{r,t} = \frac{m_{d,t}}{m_0} \times 100\% \quad (1)$$

$$M_{r,t} = \frac{M_t}{M_0} \times 100\% \quad (2)$$

$$W = \frac{(m_{w,t} - m_0)}{m_0} \times 100\% \quad (3)$$

As reference material for the degradation studies, surgical PLA was used.

Electrospinning was carried out on a custom-made spinning apparatus<sup>33</sup> consisting of a high-voltage power supply, a custom-made infusion pump, a syringe, a rotating Teflon mandrel (1.7 mm diameter), and a back electrode placed in a Faraday cage and operated in a class 1000 clean room. The synthesized TPUs were dissolved at 5 wt % in 1,1,1,3,3,3-hexafluoro-2-propanol; (HFP, Sigma-Aldrich, Vienna, Austria). The parameters for the fabrication of the grafts were  $d_1 = 8$  cm (distance needle/mandrel),  $d_2 = 1$  cm (distance mandrel/back electrode), a voltage of 10 kV, and a rotational speed of the mandrel  $n = 200$  rpm.

Tensile tests of the electrospun grafts were measured with a uniaxial tensile tester (BOSE ElectroForce LM1™ testbench system (Bose Corp. MN)) and a 10 N force transducer. Cut rings from the electrospun scaffolds of 2 mm length were soaked for 30 min in PBS buffer before testing. The rings were placed between two stainless-steel alignment pins. The samples were loaded at a crosshead speed of 10 mm min<sup>-1</sup>. Strain was calculated from the recorded elongation data and depicted as the increase in diameter from the used scaffold rings.

Suture retention was measured as described previously.<sup>33</sup> Briefly, grafts with a length of about 20 mm were clamped to one arm of the tensile testing machine (Messphysik Beta 10-2.5™, Messphysik Materials Testing GmbH, Altenmarkt, Austria) and a loop of a 7.0 polypropylene suture (Prolene™, BV 176-8, Ethicon) was placed 2 mm from the edge opposite the end of the sample. The suture loop was clamped to the other arm, which was moved with 120 mm min<sup>-1</sup> until graft failure.

The fiber morphology was assessed by scanning electron microscopy (SEM) on a JEOL JSM-5400™ (JEOL Ltd., Tokyo, Japan).

## RESULTS AND DISCUSSION

### Polymer Synthesis

In this study, different thermoplastic polyurethanes (TPUs) were synthesized by the two-step prepolymer method

(Fig. 3).<sup>24</sup> TPU synthesis was conducted using pTHF ( $\overline{M}_n = 1000 \text{ g mol}^{-1}$ ) as macrodiol (MD) in combination with the diisocyanates (DIs) HMDI, H12MDI, BIMC, and IPDI to study the effect of the different hard block symmetries as discussed in the introduction. BET was used as chain extender (CE) and  $\text{SnOct}_2$  as catalyst.<sup>39</sup> Two different stoichiometries of the components (DI:MD:CE 2:1:1 or 3:1:2) were considered to achieve ideal mechanical properties from the varying hard block content of the polymers. All polymers were obtained in yields above 80% (Fig. 3).

### Characterization of the TPUs

The molecular weight of the TPUs was determined by GPC. Table 1 displays the hard segment content, molecular weight, and polydispersity of the different investigated TPUs. HMDI\_312 was not included in detailed examinations as it was found to be too brittle in previous studies,<sup>25</sup> a result which was also reproduced in this study. The attained molecular weights and polydispersities ranged from 30 to 60 kDa and 2.1 to 2.6, respectively. These properties are in the same range as the benchmark material Pellethane<sup>®</sup>. With the exception of HMDI\_211, all other synthesized TPUs with a ratio DI:MD:CE of 2:1:1 had a rather sticky consistence and are therefore not suitable for the designated application. Respective polymers were excluded from further studies. An explanation for this finding could be given by the combined effects of low hard segment content and the higher sterical demand of alicyclic DIs that weaken the interaction between the urethane groups in the rather short hard segments.

### Differential Scanning Calorimetry

DSC experiments of the synthesized TPUs and Pellethane<sup>®</sup> as reference were performed in the temperature range from 0 to 100 °C. The melting points of the soft segments were expected in this range and taken as a measure for the degree of

**TABLE 1** Characteristics of synthesized TPUs and benchmark material Pellethane<sup>®</sup>

Polymer ID	Hard Segment Content (wt %)	Molecular Weight (kDa) <sup>a</sup>	$\overline{D}^b$
Pellethane <sup>®</sup>	- <sup>c</sup>	54.3	2.3
HMDI_211	37	46.9	2.3
H12MDI_211	44	45.0	2.4
H12MDI_312	56	57.5	2.1
BIMC_211	39	32.5	2.2
BIMC_312	52	30.8	2.5
IPDI_211	41	34.2	2.6
IPDI_312	54	40.3	2.1

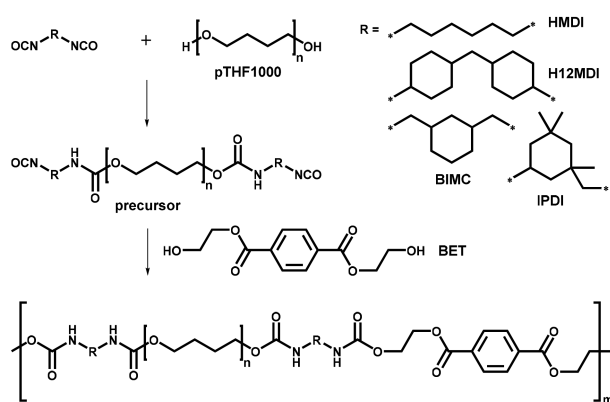
<sup>a</sup> Number average molecular weight  $\overline{M}_n$  determined by GPC analysis against PS standards in THF as mobile phase.

<sup>b</sup> Polydispersity  $\overline{D} = (\overline{M}_w / \overline{M}_n)$  with weight-average molecular weight  $\overline{M}_w$ .

<sup>c</sup> Exact composition is unknown.

microphase separation in the synthesized TPUs.<sup>40–42</sup> The obtained graphs from the DSC measurements are shown in Figure 4.

Generally, the melting point of the soft segments only shows when the soft segments are pure, that is, a high degree of segregation is attained (low amount of dissolved hard segments). In this study, only Pellethane<sup>®</sup>, HMDI\_211, and H12MDI\_312 displayed endotherms with maxima at 62.0 °C ( $1.6 \text{ J g}^{-1}$ ), 56.0 °C ( $2.5 \text{ J g}^{-1}$ ), and 66.7 °C ( $3.0 \text{ J g}^{-1}$ ), respectively, caused by the melting of soft segment domains (Fig. 4). Based on this data, phase separation of these polymers is assumed, whereas no considerable segregation was found for BIMC\_312 and IPDI\_312. The decreased diisocyanate symmetry, especially in the case of BIMC and IPDI, is expected to be the reason for the low tendency to form strong domains.<sup>24</sup>



Polymer ID	diisocyanate (DI)	macrodiol (MD)	chain extender (CE)	ratio DI:MD:CE
HMDI_211	HMDI	pTHF1000	BET	2:1:1
H12MDI_211	H12MDI	pTHF1000	BET	2:1:1
H12MDI_312				3:1:2
BIMC_211	BIMC	pTHF1000	BET	2:1:1
BIMC_312				3:1:2
IPDI_211	IPDI	pTHF1000	BET	2:1:1
IPDI_312				3:1:2

**FIGURE 3** Reaction scheme (left) and synthesized TPUs (right) using different diisocyanates. First, a macrodiol (polytetrahydrofuran with a number average molecular weight of  $1000 \text{ g mol}^{-1}$ , pTHF1000) is reacted with the diisocyanate (DI, hexamethylene diisocyanate, HMDI or 4,4'-methylene bis(cyclohexyl isocyanate), H12MDI or 1,3-bis(isocyanatomethyl)cyclohexane, BIMC or isophorone diisocyanate, IPDI). Then the chain extender bis(2-hydroxyethyl) terephthalate (BET) is added to form the high-molecular-weight polyurethanes.

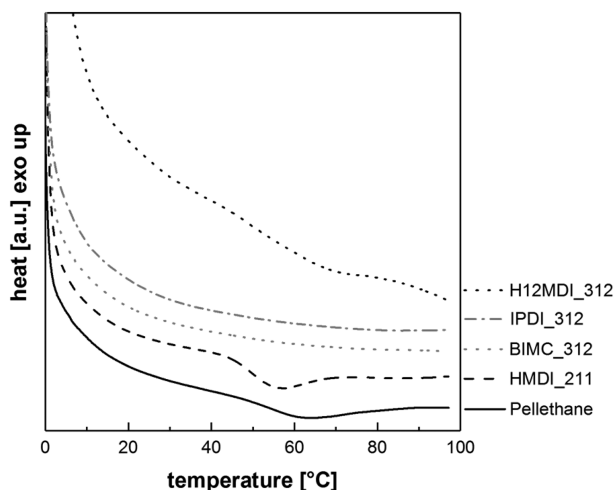


**FIGURE 4** DSC curves of synthesized TPUs with Pellethane<sup>®</sup> as reference.

### Atomic Force Microscopy

To confirm the assumed microphase separation, AFM experiments were performed. AFM cantilever-based nanoindentation measurements of solution casted material films showed that the indentation modulus of Pellethane<sup>®</sup> and H12MDI\_312 exhibits heterogeneity (Fig. 5) and ranges from 50 to 1200 MPa, which is a clear indication for the hypothesized phase segregation.

### Tensile Testing

Tensile testing was performed to investigate the mechanical properties of the TPUs in bulk. The results are shown in Table 2.

All tested TPUs showed mechanical properties typical for TPUs and comparable with the benchmark Pellethane<sup>®</sup> with the exception of BIMC\_312 (Table 2). The respective polymer generally displayed poor processability due to its sticky consistency, and showed very poor mechanical behavior. This behavior might be a consequence of the absent microphase separation as found in the DSC experiments. On the contrary, IPDI\_312 showed very good mechanical properties, comparable to the commercial benchmark material Pellethane<sup>®</sup>, although very similar thermal behavior was found for this polymer. H12MDI\_312 delivered the most promising results besides

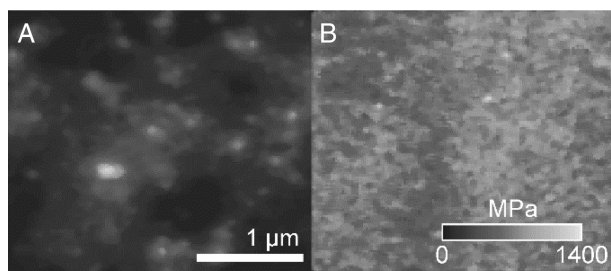


**FIGURE 5** Spatial resolution of indentation modulus of (A) Pellethane<sup>®</sup> and (B) H12MDI\_312.

**TABLE 2** Results from tensile tests of the synthesized TPUs

TPU	$E^a$ [MPa]	$S^a$ [MPa]	$\epsilon_b^a$ (%)
Pellethane <sup>®</sup>	14 ± 3	43 ± 8	998 ± 130
HMDI_211	55 ± 12	21 ± 5	1285 ± 202
H12MDI_312	28 ± 8	49 ± 3	818 ± 26
BIMC_312	0.5 ± 0.3	2.8 ± 0.5	3124 ± 378
IPDI_312	12 ± 2	48 ± 4	1186 ± 29

<sup>a</sup>  $E$ , elastic modulus;  $S$ , tensile strength;  $\epsilon_b$ , strain at break.

IPDI\_312. H12MDI\_312 displayed an elastic modulus twice as high as for Pellethane<sup>®</sup>, and considerably higher strength compared to the linear aliphatic analog HMDI\_211 as described in literature.<sup>28</sup> Apart from all other structural considerations, it must be considered that H12MDI\_312 had a higher hard segment content compared to HMDI\_211 (56 vs. 44 wt %). However, as mentioned before, the according polymer HMDI\_312 was reproducibly found to be too brittle for the solution casting process owing to an excessive hard segment content.<sup>25</sup> It seems that the broken symmetry (owing to the conformational isomerization of the cyclohexyl-rings) and increased steric demand of the H12MDI urethane moieties,<sup>24,31</sup> combined with the raised hard segment content give a good trade-off and result in a more balanced structure. Therefore, more favorable mechanical properties were obtained for H12MDI\_312 than for the corresponding HMDI\_312 material.

### DMTA Testing

DMTA measurements were performed to acquire additional information about the thermal behavior of the TPUs. In this study,  $T_g$  was determined at the maximum of the loss factor ( $\tan \delta$ ). The DMTA curves are shown in Figure 6 and the results are listed in Table 3.

The value for  $T_g$  found for Pellethane<sup>®</sup> is higher than reported by the manufacturer ( $T_g = -42$  °C/DSC),<sup>43</sup> However, it is in the same range. The  $T_g$  values are predominantly determined

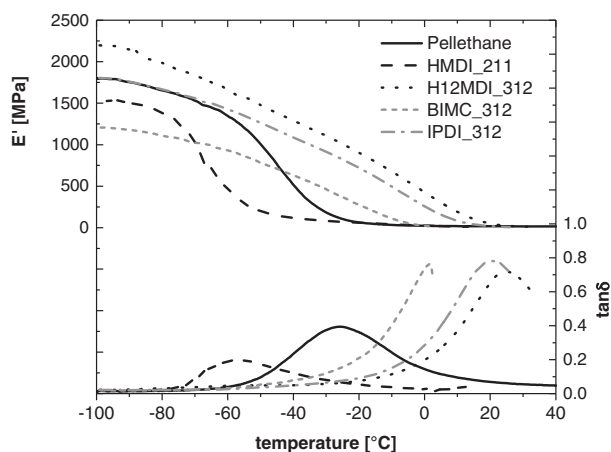


**FIGURE 6** DMTA curves of synthesized TPUs: storage modulus ( $E'$ ) and loss factor ( $\tan \delta$ ).

**TABLE 3** DMTA measurement results: glass transition temperatures ( $T_g$ s) of soft segments from  $\tan \delta$  data and storage moduli ( $E'$ ) at room temperature

TPU	$T_g$ [°C]	$E'$ (21 °C) (MPa)
Pellethane®	$-26 \pm 1$	$16 \pm 1$
HMDI_211	$-59 \pm 2$	$6 \pm 1$
H12MDI_312	$25 \pm 1$	$48 \pm 8s$
BIMC_312	$17^a$	$-^b$
IPDI_312	$23 \pm 4$	$25 \pm 13$

<sup>a</sup> Only data from a single measurement available owing insufficient specimen quality.

<sup>b</sup> Sample failure before room temperature.

by the soft segment mobility. For the TPU based on linear aliphatic HMDI, the value for the  $T_g$  was significantly lower than for Pellethane®, which might result from a lower molecular weight of the soft segment in Pellethane® (the exact information on the molecular weight of the soft segment was not available). The  $T_g$  increases fast with increasing concentration of hard segment in the TPU. This is due to the increased constraints introduced by an increasing hard segment concentration, which hinder the onset of the soft segment mobility.<sup>41</sup> As already found in DSC measurements, the TPUs with alicyclic urethane moieties are most affected by this process and their  $T_g$  values are shifted considerably toward higher temperatures.<sup>44</sup> H12MDI\_312 with the most bulky groups (two cyclohexyl rings) showed the highest  $T_g$  among the tested polymers. IPDI\_312, having branched methyl groups, however, displays an increased flexibility due to one primary isocyanate group. Finally, BIMC\_312, based on the most flexible alicyclic diisocyanate with two primary isocyanate groups, displayed the lowest  $T_g$  of all alicyclic derivatives. All TPUs showed a  $T_g$  below body temperature and therefore are expected to show elastomeric properties after implantation into mammals, which is an important feature for the quality of polymers in soft-tissue engineering.<sup>44</sup>

The tendency of the storage modulus ( $E'$ ) at room temperature was also applicable by DMTA experiments. Especially for the TPUs synthesized with alicyclic diisocyanates, high errors were found for these measurements, which were mainly attributed to the fact that these polymers have their glass transitions near room temperature. However, most of the results are in good correlation with the values found for the elastic modulus ( $E$ ) in tensile testing (Tables 2 and 3).

### Degradation and Water Uptake

Degradation characteristics<sup>45–48</sup> of materials employed as scaffolds for the remodeling of natural tissue are of central importance for regenerative medicine. The mechanism for the degradation of many biomaterials and the synthesized TPUs in this study is the cleavage of ester bonds.<sup>49</sup>

Here, an accelerated degradation process at elevated temperatures (90 °C) in PBS buffer solution (pH 7.4) is used to reduce

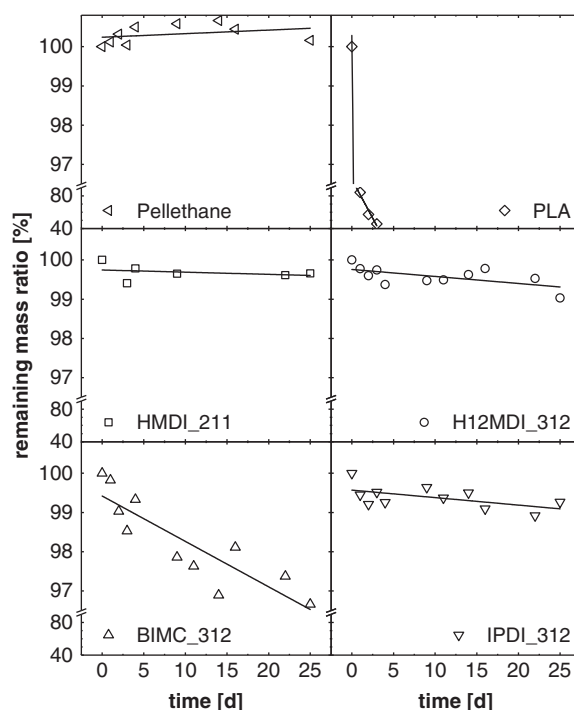
experimental time.<sup>50</sup> Pellethane® and surgical PLA were used as reference materials.

During the degradation experiments, we found that PLA eroded very fast and was already fully degraded after 4 days (Fig. 7). In contrast, Pellethane® did not show any traces of degradation over the monitored time range, as expected.<sup>25</sup> The increase in mass (as displayed in Fig. 7) in case of Pellethane® is assumed to be an effect of deposition of salts from PBS solution which could not sufficiently be removed during the washing procedure.

The TPUs in this study were designed to be hard segment degradable as cleavable bonds were introduced by the chain extender.<sup>25</sup> Hydrophilicity and access to the cleavable groups are the most important factors for degradation.

The two polymers based on H12MDI and IPDI in the hard segment, which displayed increased mechanical properties, degraded slightly faster than the HMDI-based TPU (Fig. 7 and Table 4). There was a slight difference between polymers containing H12MDI- and IPDI-derived hard segments. The IPDI-based TPU degraded slightly faster than the material synthesized with H12MDI as seen by the mass erosion velocity in Table 4. Generally, mass erosion followed the same trend as the water uptake of the polymers (Fig. 8). This is an indication for the impact of hydrophilicity on the degradability of the polymers.

The increased hydrophilicity of the monocyclohexyl urethane moiety derived from IPDI compared to the dicyclohexyl group

**FIGURE 7** Mass erosion of synthesized TPUs during degradation experiments: surgical poly(lactic acid) (PLA) and nondegradable Pellethane® as references.

**TABLE 4** Mass erosion velocities of synthesized TPUs derived from linear fits of mass erosion curves of degradation experiments

TPU	Mass Erosion Velocity [ $10^{-2}\%$ d $^{-1}$ ]
Pellethane®	0.92
PLA	-1900
HMDI_211	-0.56
H12MDI_312	-1.79
BIMC_312	-11.6
IPDI_312	-1.91

of H12MDI-based TPU is supposed to be the reason for the different degradation behavior. Both had a higher hydrophilic hard segment concentration compared to HMDI-based TPU, and therefore degraded faster than the linear aliphatic diisocyanate containing material.

The TPU synthesized from the cyclohexyl-based BIMC showed the fastest erosion rate. This is supposedly due to the combined effects of the rather low molecular weight and the low microphase separation of the polymer, making water permeation into the space between the polymer chains easier. To decipher the degradation mechanism, GPC measurements of selected samples were conducted (Fig. 9).

A comparison of the data for mass erosion of BIMC\_312 (Fig. 7) and the decrease of molecular weight (Fig. 9) makes a bulk erosion mechanism most likely, which is often observed for degradable polymers with cleavable ester bonds.<sup>45</sup>

### Electrospinning

Electrospinning enables the production of seamless, nonwoven, fibrous structures that can mimic the ECM and possess a

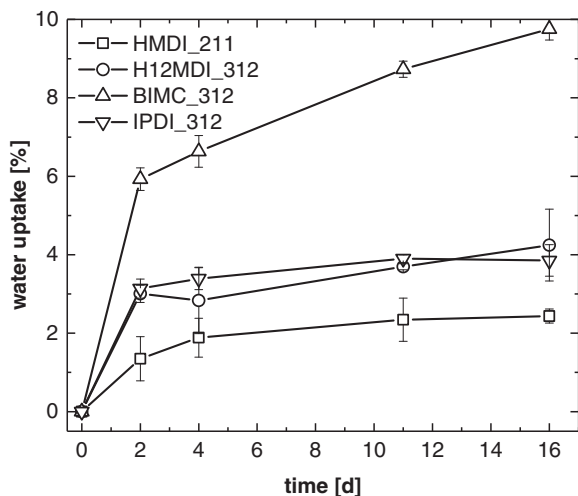


**FIGURE 8** Water uptake of synthesized TPUs during degradation experiments.

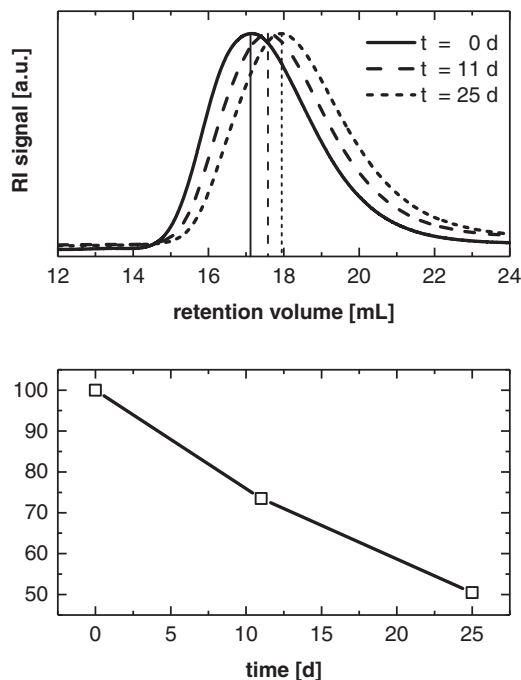


**FIGURE 9** Gel permeation chromatography eluograms (top) and molecular weight of samples of BIMC\_312 after different degradation times: a steady decrease in the molecular weight indicates a bulk erosion mechanism.

large porosity and large surface-to-volume ratio with interconnected pores.

Apart from the TPU synthesized with HMDI, the polymer based on H12MDI was also chosen for an electrospinning study, because both materials showed mechanical properties comparable to the benchmark Pellethane®. The electrospun scaffolds had an internal diameter of 1.7 mm and a wall thickness of 80–90  $\mu\text{m}$ . Scanning electron microscopy images of the grafts from H12MDI\_312 were taken and compared to HMDI\_211 as shown in Figure 10.

The grafts from TPU with the linear aliphatic hard segment showed well-separated fibers with diameters of  $1.39 \pm 0.47 \mu\text{m}$  (mean  $\pm$  standard deviation), whereas the fibers spun from alicyclic hard segment containing TPU showed a fused structure and smaller pore sizes with fiber diameters of  $0.87 \pm 0.34 \mu\text{m}$  (mean  $\pm$  standard deviation). Manifold parameters influence the fiber quality of ES processes. Important parameters originate from the polymer solution, including viscosity, surface tension, conductivity, and so forth.<sup>51</sup> In this preliminary ES study, these parameters could not be controlled independently. In fact, the polymer solution with H12MDI\_312 had visually obvious higher viscosity compared to the HMDI\_211 solution, which can be explained by the different molecular weights of the polymers as reported above. To establish uniform polymer jets, a higher pumping rate in case of HMDI\_211 was necessary to compensate the difference in solution viscosities.<sup>52</sup>



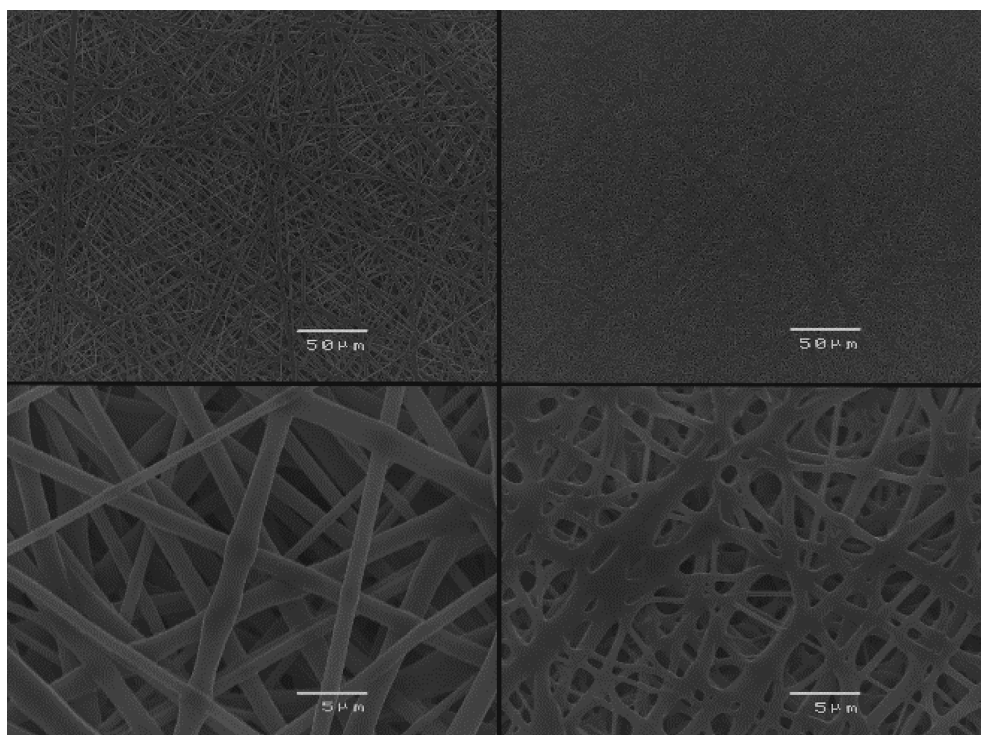


**FIGURE 10** Scanning electron microscopy images of electrospun grafts synthesized with different diisocyanates: HMDI (left) and H12MDI (right).

A comparison of the typical tensile test curves of electrospun grafts is shown in Figure 11. The tensile strengths of HMDI<sub>211</sub> and H12MDI<sub>312</sub> are below the values of Pellethane<sup>®</sup> grafts but exceed the strength of an abdominal rat aorta<sup>33</sup> (Fig. 11). Besides the tensile tests described above, suture tear retention was also measured. With  $2.8 \pm 0.2$  N, the suture tear retention force of H12MDI<sub>312</sub> lies above the values of the benchmark material Pellethane<sup>®</sup> (electrospun, as reported in literature<sup>33</sup>) and abdominal rat aorta. The good

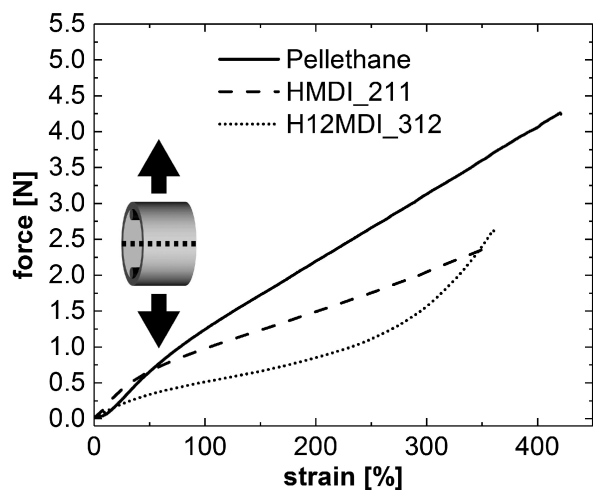


**FIGURE 11** Results of tensile tests on electrospun grafts made of Pellethane<sup>®</sup>, HMDI<sub>211</sub>, and H12MDI<sub>312</sub>.

performance of H12MDI in this case is supposedly a side effect of the fused fibers as seen in Figure 10.

## CONCLUSIONS

In this study, new degradable thermoplastic polyurethanes with enhanced mechanical properties suitable for electrospinning were synthesized. The commercially available TPU Pellethane<sup>®</sup> 2363-80A, which has already shown good performance as electrospun vascular grafts in rats, was used as a reference material and structural template. The aromatic diisocyanate-based hard segment of Pellethane<sup>®</sup> was exchanged by commercially available linear aliphatic and alicyclic diisocyanates (hexamethylene diisocyanate (HMDI), more rigid alicyclic 4,4'-methylenebis(cyclohexylisocyanate) (H12MDI), 1,3-bis(isocyanatomethyl)cyclohexane (BIMC), and isophorone diisocyanate (IPDI)) to avoid the formation of potentially toxic aromatic amine-derived degradation products. To introduce degradability, the aliphatic chain extender butanediol of Pellethane<sup>®</sup> was exchanged by a cleavable ester, bis(2-hydroxyethyl) terephthalate.

As proposed, the symmetry and flexibility of the used diisocyanates had tremendous impact on the mechanical properties of the TPUs as found in tests with solution-casted films. For the linear aliphatic HMDI, an optimum ratio of components (diisocyanate:macrodiol:chain extender) was found to be 2:1:1. An even higher hard segment content (component ratio of 3:1:2) generally led to brittle materials. In case of the polymers with alicyclic hard segment moieties, however, a higher hard segment content was necessary (i.e., a component

ratio of 3:1:2) to obtain TPUs with sufficient mechanical properties. We concluded that the increasing broken symmetry in the hard segments demanded higher hard segment weight ratios for similar mechanical performance. Especially the polymer with BIMC-derived urethane moieties showed very poor mechanical properties, most probably due to the less favorable 1,3-disubstitution of the cyclohexane ring. In contrast to BIMC, the TPUs containing H12MDI- and IPDI-derived urethane moieties displayed comparable mechanical properties to commercial Pellethane®.

Polymers synthesized in this study displayed bulk degradation characteristics during hydrolytic degradation experiments. Mass erosion of 3–4 wt % was observed during a degradation time of 25 days at 90 °C in PBS solution. Pellethane® showed no degradation in a reference degradation experiment. An interesting finding is the opposing trends of mechanical stability and degradability. The material with very poor mechanical properties, BIMC\_312, had by far the fastest degradation behavior (about 10 times higher mass erosion compared to all other degradable TPUs). We conclude that this is a direct consequence of the weak interaction of the polymer chains in the hard segments, which results in a better accessibility of the cleavable bonds in the hard segments for water and therefore degradation is accelerated.

DSC measurements indicated thermal transitions from 44 to 84 °C for Pellethane® and HMDI\_211, and to a minor extent for H12MDI\_312, which suggests a higher semi-crystallinity in the hard segments. This is in agreement with the DMTA measurements. The hypothesized microphase segregation was confirmed by means of AFM cantilever-based nanoindentation measurements.

From these data, we expect that the aforementioned difference in the mechanical properties is mainly caused by the difference in phase segregation typical for this type of polymer: The steric effects of varying isocyanate components in the hard block influence the effectiveness of hydrogen bonding in the hard block. This directly determines the ability for microphase segregation and therefore the mechanical stability of the material.

Both TPUs synthesized with HDMI and H12MDI could be spun to grafts with different fiber appearance. The HDMI-based material showed well-separated fibers with a high graft wall porosity, whereas the H12MDI-based TPUs displayed fused fibers which is supposed to contribute to the excellent graft strength and suture tear resistance.

In summary, we were able to present in this study a portfolio of novel materials with tunable properties for electrospun biodegradable TPUs with high potential for application in vascular tissue engineering. Emphasis on the fine tuning of the optimal TPU properties and ES parameters for VTE purposes will be placed in further experiments.

#### ACKNOWLEDGMENTS

The authors would like to thank the Austrian Wirtschaftsservice (AWS, PRIZE Prototype funding project “Aliphatische

Thermoplastische Urethan-Elastomere für die Herstellung von elektrogenen bioabbaubaren Blutgefäßersatzmaterialien”, number P1405063), the Techniker-Cercle (project “New material for the manufacture of artificial blood vessels”), and the Ludwig Boltzmann Society for financial support of this work.

#### REFERENCES

- H. M. Nugent, E. R. Edelman, *Circ. Res.* **2003**, *92*, 1068.
- C. Kasper, *Chem. unserer Zeit* **2005**, *39*, 394.
- S.-W. Ha, E. Wintermantel, G. Maier, In *Medizintechnik: Life Science Engineering*, E. Wintermantel, S.-W. Ha Eds., Springer Berlin Heidelberg, Berlin, Heidelberg, **2009**, p. 219.
- R. Langer, J. Vacanti, *Science* **1993**, *260*, 920.
- C. T. Laurencin, A. M. A. Ambrosio, M. D. Borden, J. J. A. Cooper, *Annu. Rev. Biomed. Eng.* **1999**, *1*, 19.
- L. G. Griffith, G. Naughton, *Science* **2002**, *295*, 1009.
- M. Spagnuolo, L. Liu, *ISRN Nanotechnol.* **2012**, *2012*, 11.
- W. Ho, B. Tawil, J. C. Y. Dunn, B. M. Wu, *Tissue Eng.* **2006**, *12*, 1587.
- A. Hasan, A. Memic, N. Annabi, M. Hossain, A. Paul, M. R. Dokmeci, F. Dehghani, A. Khademhosseini, *Acta Biomater.* **2014**, *10*, 11. <https://doi.org/10.1016/j.actbio.2013.08.022>.
- S. A. Sell, M. J. McClure, K. Garg, P. S. Wolfe, G. L. Bowlin, *Adv. Drug Del. Rev.* **2009**, *61*, 1007.
- C. Grasl, H. Bergmeister, M. Stoiber, H. Schima, G. Weigel, *J. Biomed. Mater. Res. A* **2010**, *93A*, 716.
- J. W. Shin, Y. J. Lee, S. J. Heo, S. A. Park, S.-H. Kim, Y. J. Kim, D.-H. Kim, J.-W. Shin, *J. Biomater. Sci. Polym. Ed.* **2009**, *20*, 757.
- T. J. Sill, H. A. von Recum, *Biomaterials* **2008**, *29*, 1989.
- R. Chandra, R. Rustgi, *Prog. Polym. Sci.* **1998**, *23*, 1273.
- W. Wu, R. A. Allen, Y. Wang, *Nat. Med.* **2012**, *18*, 1148.
- S. J. Kew, J. H. Gwynne, D. Enea, R. Brookes, N. Rushton, S. M. Best, R. E. Cameron, *Acta Biomater.* **2012**, *8*, 3723.
- D. W. Courtman, B. F. Errett, G. J. Wilson, *J. Biomed. Mater. Res.* **2001**, *55*, 576.
- Y. Song, J. W. H. Wennink, M. M. J. Kamphuis, I. Vermes, A. A. Poot, J. Feijen, D. W. Grijpma, *J. Biomed. Mater. Res. A* **2010**, *95A*, 440.
- B. Tschoeke, T. C. Flanagan, S. Koch, M. S. Harwoko, T. Deichmann, V. Ellå, J. S. Sachweh, M. Kellomäki, T. Gries, T. Schmitz-Rode, S. Jockenhoevel, *Tissue Eng. A* **2009**, *15*, 1909.
- D. B. Khadka, D. T. Haynie, *Nanomedicine* **2012**, *8*, 1242.
- A. Sarasam, S. V. Madhally, *Biomaterials* **2005**, *26*, 5500.
- E. Carletti, A. Motta, C. Migliaresi, 3D Cell Culture: Methods and Protocols. In , W. J. Haycock Ed., Humana Press, Totowa, NJ, **2011**, p. 17.
- Y. Li, J. Rodrigues, H. Tomas, *Chem. Soc. Rev.* **2012**, *41*, 2193.
- I. Yilgör, E. Yilgör, G. L. Wilkes, *Polymer* **2015**, *58*, A1.
- S. Baudis, S. C. Ligon, K. Seidler, G. Weigel, C. Grasl, H. Bergmeister, H. Schima, R. Liska, *J. Polym. Sci. Part A: Polym. Chem.* **2012**, *50*, 1272.
- G. Soldani, P. Losi, M. Bernabei, S. Burchielli, D. Chiappino, S. Kull, E. Briganti, D. Spiller, *Biomaterials* **2010**, *31*, 2592.
- H. Bergmeister, N. Seyidova, C. Schreiber, M. Strobl, C. Grasl, I. Walter, B. Messner, S. Baudis, S. Fröhlich, M. Marchetti-Deschmann, M. Griesser, M. di Franco, M. Krssak, R. Liska, H. Schima, *Acta Biomater.* **2015**, *11*, 104.
- D.-K. Lee, H.-B. Tsai, *J. Appl. Polym. Sci.* **2000**, *75*, 167.
- S. H. Kenyon, J. Bhattacharyya, C. J. Benson, P. L. Carmichael, *Toxicology* **2004**, *196*, 65.

- 30** S. Ambs, H.-G. Neumann, *Toxicol. Appl. Pharmacol.* **1996**, *139*, 186.
- 31** T. Padmavathy, K. S. V. Srinivasan, *J. Polym. Sci. Part A: Polym. Chem.* **2002**, *40*, 1527.
- 32** W. L. F. Armarego, C. L. L. Chai, *Purification of Laboratory Chemicals (Fifth Edition)*, Butterworth-Heinemann, Burlington, **2003**, p. 80.
- 33** H. Bergmeister, C. Schreiber, C. Grasl, I. Walter, R. Plasenzotti, M. Stoiber, D. Bernhard, H. Schima, *Acta Biomater.* **2013**, *9*, 6032.
- 34** D. Cohn, A. Hotovely-Salomon, *Polymer* **2005**, *46*, 2068.
- 35** D. Cohn, A. Hotovely Salomon, *Biomaterials* **2005**, *26*, 2297.
- 36** J. L. Hutter, J. Bechhoefer, *Rev. Sci. Instrum.* **1993**, *64*, 1868.
- 37** O. G. Andriotis, W. Manuyakorn, J. Zekonyte, O. L. Katsamenis, S. Fabri, P. H. Howarth, D. E. Davies, P. J. Thurner, *J. Mech. Behav. Biomed. Mater.* **2014**, *39*, 9.
- 38** A. Fischer-Cripps, *Nanoindentation*, New York, NY, Springer, **2002**.
- 39** M. V. Pandya, D. D. Deshpande, D. G. Hundiwale, *J. Appl. Polym. Sci.* **1986**, *32*, 4959.
- 40** J. W. C. Van Bogart, D. A. Bluemke, S. L. Cooper, *Polymer* **1981**, *22*, 1428.
- 41** A. Eceiza, M. D. Martin, K. de la Caba, G. Kortaberria, N. Gabilondo, M. A. Corcuera, I. Mondragon, *Polym. Eng. Sci.* **2008**, *48*, 297.
- 42** T. W. Son, D. W. Lee, S. K. Lim, *Polym. J.* **1999**, *31*, 563.
- 43** In Lubrizol LifeSciences Technical Datasheet, **2016**.
- 44** C. Zhang, N. Zhang, X. Wen, *J. Biomed. Mater. Res. A* **2007**, *82A*, 637.
- 45** F. V. Burkersroda, L. Schedl, A. Göpferich, *Biomaterials* **2002**, *23*, 4221.
- 46** A. Göpferich, *Macromolecules* **1997**, *30*, 2598.
- 47** A. Göpferich, *Biomaterials* **1996**, *17*, 103.
- 48** J. S. Soares, P. Zunino, *Biomaterials* **2010**, *31*, 3032.
- 49** L. S. Nair, C. T. Laurencin, *Prog. Polym. Sci.* **2007**, *32*, 762.
- 50** X. Yuan, A. F. T. Mak, K. Yao, *Polym. Degrad. Stab.* **2002**, *75*, 45.
- 51** N. Amariei, L. R. Manea, A. P. Berteau, A. Berteau, A. Popa, *IOP Conf. Ser. Mater. Sci. Eng.* **2017**, *209*, 012092.
- 52** L. Du, H. Xu, Y. Zhang, F. Zou, *Fibers Polym.* **2016**, *17*, 751.